

Implication of nano-Hertz stochastic gravitational wave background on ultralight axion particles and fuzzy dark matter

Jing Yang,¹ Ning Xie,¹ and Fa Peng Huang^{1,*}

¹*MOE Key Laboratory of TianQin Mission, TianQin Research Center for Gravitational Physics & School of Physics and Astronomy, Frontiers Science Center for TianQin, Gravitational Wave Research Center of CNSA, Sun Yat-sen University (Zhuhai Campus), Zhuhai 519082, China*

Recently, the Hellings Downs correlation has been observed by different pulsar timing array (PTA) collaborations, such as NANOGrav, European PTA, Parkes PTA, and Chinese PTA. These PTA measurements of the most precise pulsars within the Milky Way show the first evidence for the stochastic gravitational wave background of our Universe. We study the ultralight axion interpretation of the new discovery by investigating the gravitational wave from axion transitions between different energy levels of the gravitational atoms, which are composed of cosmic populated Kerr black holes and their surrounding axion clouds formed from the superradiant process. We demonstrate that this new observation naturally admits an ultralight axion interpretation around 2×10^{-21} eV, which is consistent with the typical fuzzy dark matter.

Introduction.—Recently, the expected Hellings-Downs [1] curve has finally been observed by the global pulsar timing array (PTA) experiments including NANOGrav [2], European PTA (EPTA) [3], Parkes PTA (PPTA) [4], and Chinese PTA (CPTA) [5], which provide strong evidence for the detection of stochastic gravitational wave background (SGWB). The observation of SGWB has wide and deep implications for astrophysics and particle cosmology. Especially, the PTA measurement of SGWB opens new windows to explore the new physics beyond the standard model [6, 7]. In this work, we focus on the implication of the new observation to the ultralight axion [8] or axion-like particles [9] (in this letter, we simply use axion to represent both axion and axion-like particle), which could provide a natural solution to the strong CP problem and a well-motivated dark matter (DM) candidate [10, 11]. Motivated by the current situation of DM search, recently more and more studies have focused on ultralight bosons, such as ultralight axions or dark photons. As pseudo scalar particles, ultralight axion particles can form Bose-Einstein condensation and further form dense axion objects, like axion stars or axion clusters. Especially, the so-called axion cloud can be formed from the superradiant process around Kerr black hole (BH) [12–15]. Once the axion cloud is formed, abundant signals could be produced. For example, the axion cloud can be a promising gravitational wave (GW) source [16–21], which can be used to explore the properties of axion particles [22–26].

In this letter, we fit the first observation of the nano-Hertz SGWB with the ultralight axion particles by considering the transition process of the bound state of the axion cloud and Kerr BH, which is ignored in the previous study. We introduce the gravitational atom as the new type of interpretation of nano-Hertz SGWB and calculate the GW radiation power from the isolated gravitational atom. Further, considering the universal BH population, we give the expected SGWB for the ultralight axion in

the mass range $[10^{-21}, 10^{-19}]$ eV, and compare it with the new PTA data and SGWB from super-massive black holes (SMBH) binaries by Bayesian analysis.

The axion cloud and gravitational atom from superradiance around Kerr black hole.—From general relativity, the Penrose process [12] can naturally form the axion cloud around the Kerr BHs since there exists an ergosphere between the static limit surface and the event horizon. From quantum field theory, the axion field is described by the Klein-Gordon equation in the Kerr metric. Matching radial solutions at infinity (confluent hypergeometric function) and the event horizon (hypergeometric function) together, it occurs exponential growth solution when the Compton length is larger than the BH size [15, 27]. The axion cloud extracts energy and angular momentum from the Kerr BH. Similar to the atom, the BH and its axion cloud can form the so-called gravitational atom. Once the gravitational atom is formed, various types of GW signals can be produced from axions annihilating to gravitons or transitions between different energy levels of the gravitational atom. The GWs from axion clouds around the SMBHs could contribute to the signal of nano-Hertz SGWB, which is detectable through PTA experiments, as shown in Fig. 1. There distribute a large number of SMBHs in our Universe. And if their initial spin is greater than the critical value that triggers the superradiant process, the gravitational atoms consisting of the condensed axion cloud and SMBH can be generated. Further, the axion transition from an excited energy level to a ground energy level is possible through the GW radiation. If the occupation numbers of the levels are sufficiently large, the GW effect could be detectable. We find that the energy-level transition process naturally generates SGWB falling in the nano-Hertz frequency band. Therefore, the SGWB observation can help to explore the ultralight axion DM.

The radiation power of the isolated gravitational atom.—We denote the BH, axion mass as M_b ,

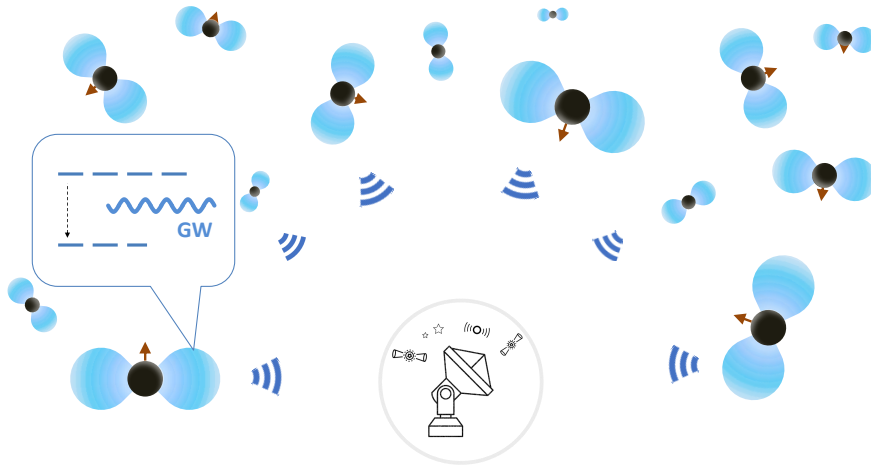


Figure 1. The cosmic populated SMBHs dressed with the axion cloud as a natural source of nano-Hertz SGWB. The energy-level transition process can radiate GWs continuously, which naturally fall in the nano-Hertz frequency band. Consequently, the PTA could detect this new source which provides a new approach to probe ultralight axion DM and isolated BHs.

and m_a respectively. The fine structure constant of the gravitational atom is $\alpha = GM_b m_a$ where G is Newton's constant. When the superradiant condition is satisfied, the occupation number grows as

$$\left. \frac{dN}{dt} \right|_{\text{sr}} = \Gamma_{\text{sr}} N, \quad (1)$$

where Γ_{sr} is the superradiant rate. The superradiant rate of different energy levels is calculated numerically following the method used in Ref. [25]. The results of energy levels $l = m = n - 1$ with $J = 0.99 GM_b^2$ is shown in the Fig 2., where n, l, m are the principal, orbital, and magnetic quantum numbers, J is the spin angular momentum of the BH. The superradiant time scale is

$$\tau_{\text{sr}} = 1/\Gamma_{\text{sr}} = 1.57 \times 10^5 \text{ yr} \left(\frac{M_b}{10^8 M_\odot} \right)^{-1}. \quad (2)$$

To get stronger SGWB signal, more axions are needed to occupy the initial state energy level for the transition process. The energy levels of the transition process $|644\rangle \rightarrow |544\rangle$ have the smallest principle and orbital quantum numbers when the superradiant rate of the initial state energy level is larger than the final state energy level. For the transition process with higher energy levels, the corresponding superradiant rate is slower compared with the $|644\rangle \rightarrow |544\rangle$ process [17]. So we consider the dominant transition process $|644\rangle \rightarrow |544\rangle$ in this work. We take the superradiant rate of the energy level $|644\rangle$ as $\Gamma_{544}/\Gamma_{644} = 0.9$ for simplicity [23]. Thus the numbers of axions occupying the energy levels have the relation

$N_5 = N_6^{0.9}$ during the superradiant process where N_5 and N_6 are axion numbers of the states $|544\rangle$ and $|644\rangle$ respectively.

We can see from Fig. 2, the superradiant process is dominated by energy levels with $l = m = 4$ when $1.38 \lesssim \alpha \lesssim 1.85$. The relevant scales are the accretion time scale t_S , the superradiant time scale $\tau_{\text{sr}} = 1/\Gamma_{644}$ and the age of the universe t_0 . The time of the superradiant process must be smaller than the t_S and t_0 . If the superradiant rate is fast enough, the superradiant situation is saturated with the total axion number

$$N_{\text{max}} \simeq \frac{GM_b^2}{m} \Delta a \simeq 0.01 GM_b^2, \quad (3)$$

where $\Delta a = \Delta J/GM_b^2 \simeq 0.04$ is the difference between the initial and final BH spin with the initial spin $J = 0.99 GM^2$. We consider the axion number of the energy level $|644\rangle$ as $N_6 \simeq \min[N_{\text{max}}, \exp(\min[t_0, t_S] * \Gamma_{644})]$ when the superradiant process is terminated.

The energy spectrum of the gravitational atom is given by

$$\omega_n \approx m_a \left(1 - \frac{\alpha^2}{2n^2} \right), \quad (4)$$

and the frequency split of the two states is

$$\Delta\omega = \frac{11}{1800} \alpha^2 m_a. \quad (5)$$

The transition rate of the process $|644\rangle \rightarrow |544\rangle$ is given

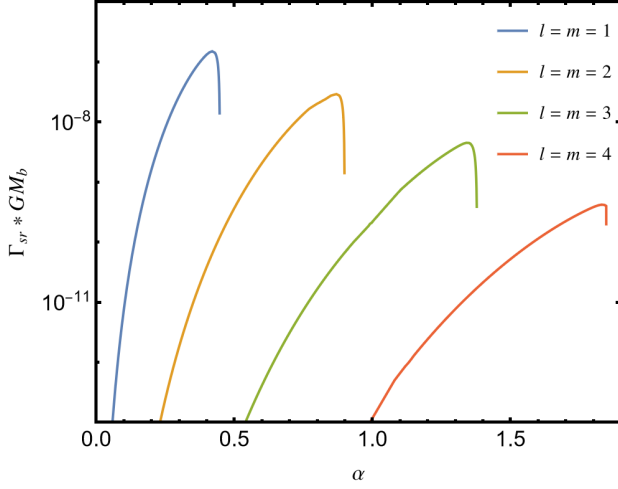


Figure 2. The superradiant rate of different energy levels in the unit $1/GM_b$. The result is calculated with $l = m = n - 1$ and the BH spin $J = 0.99 GM_b^2$.

by [23],

$$\left. \frac{dN_6}{dt} \right|_{\text{tr}} \approx 3 \times 10^{-7} N_1 N_0 \frac{G\alpha^9}{r_g^3}, \quad (6)$$

where $r_g = GM_b$ is the gravitational radius of the BH. If the axion annihilation process is considered after superradiance is terminated, the axion numbers evolve as

$$\frac{dN_6}{dt} = -\Gamma_{\text{tra}} N_5 N_6 - \Gamma_{\text{ann},6} N_6^2, \quad (7)$$

$$\frac{dN_5}{dt} = \Gamma_{\text{tra}} N_5 N_6 - \Gamma_{\text{ann},5} N_5^2, \quad (8)$$

where the transition rate $\Gamma_{\text{tra}} = 3 \times 10^{-7} G\alpha^9/r_g^3$ can be read from Eq. (6) and $\Gamma_{\text{ann},5}(\Gamma_{\text{ann},6})$ is the annihilation rate of the $|544\rangle$ ($|644\rangle$) state. The Γ_{ann} can be estimated as [17]

$$\Gamma_{\text{ann}} \approx 10^{-10} \left(\frac{2\alpha}{l} \right)^p \frac{G}{r_g^3}, \quad (9)$$

where $p = 17$ for $l = 1$ and $p = 4l + 11$ for $l > 1$. Since $\Gamma_{\text{ann}} N_5 \ll \Gamma_{\text{tra}} N_6$, we can neglect the annihilation process at the energy level $|544\rangle$. For the evolution of the energy level $|644\rangle$, we need to consider different cases:

1. $\Gamma_{\text{ann}} N_6(t_*) > \Gamma_{\text{tra}} N_5(t_*)$, where t_* is the time when superradiance is terminated. The annihilation process dominated the evolution of the axion number in the first stage,

$$\frac{dN_6}{dt} \simeq -\Gamma_{\text{ann}} N_6^2, \quad (10)$$

$$\frac{dN_5}{dt} = \Gamma_{\text{tra}} N_5 N_6, \quad (11)$$

the solution is

$$N_6(t_* + t) = \frac{N_6(t_*)}{1 + \Gamma_{\text{ann}} N_6(t_*) t}, \quad (12)$$

$$N_5(t_* + t) = N_5(t_*) (1 + \Gamma_{\text{ann}} N_6(t_*) t)^{\Gamma_{\text{tra}}/\Gamma_{\text{ann}}}. \quad (13)$$

Then we can solve the equation $\Gamma_{\text{ann}} N_6(t_* + t) = \Gamma_{\text{tra}} N_5(t_* + t)$ to get the time length t_a of the first stage, we obtain

$$t_a = (N_6(t_*) \Gamma_{\text{ann}})^{-\frac{\Gamma_{\text{tra}}}{\Gamma_{\text{tra}} + \Gamma_{\text{ann}}}} (N_5(t_*) \Gamma_{\text{tra}})^{-\frac{\Gamma_{\text{ann}}}{\Gamma_{\text{tra}} + \Gamma_{\text{ann}}}} - \frac{1}{N_6(t_*) \Gamma_{\text{ann}}}. \quad (14)$$

Then the second stage is that the transition process dominates the evolution of axion number. Since $N_6(t_* + t_a) \gg N_5(t_* + t_a)$, we can roughly take N_6 unchanged in this stage. Thus the occupation number of the state $|544\rangle$ evolves as $N_5(t_* + t_a + t) = N_5(t_* + t_a) e^{\Gamma_{\text{tra}} N_6(t_* + t_a) t}$. The time length of the second stage is estimated as $t_b = \ln(N_6(t_* + t_a)/N_5(t_* + t_a)) / (\Gamma_{\text{tra}} N_6(t_* + t_a))$. The gravitational radiation time scale is $\tau_{\text{GW}} = t_a + t_b$.

2. $\Gamma_{\text{ann}} N_6(t_*) < \Gamma_{\text{tra}} N_5(t_*)$, the transition process would dominate the evolution. The axion number of the energy level $|544\rangle$ is $N_5(t_* + t) = N_5(t_*) e^{\Gamma_{\text{tra}} N_6(t_*) t}$. The gravitational radiation time scale is estimated as $\tau_{\text{GW}} = \ln(N_6(t_*)/N_5(t_*)) / (\Gamma_{\text{tra}} N_6(t_*))$.

The radiation power of the transition process is obtained as

$$P = -\frac{dE}{dt} = \frac{dN_5(t)}{dt} \Delta\omega. \quad (15)$$

The total radiation energy of GW from axion transitions between different energy levels is

$$E_t(t) = (N_5(t) - N_5(t_*)) \Delta\omega. \quad (16)$$

Stochastic gravitational wave with cosmic black hole population.— The distribution of SMBHs is essential to calculate the spectra of the SGWB. For isolated BHs, the number density in the comoving volume is estimated as [28, 29]

$$\frac{dn}{d \log_{10} M_b} = 0.002 \left(\frac{M_b}{3 \times 10^6 M_\odot} \right)^{0.3} \text{Mpc}^{-3}, \quad (17)$$

where M_\odot is the solar mass. This formula is valid for $10^4 M_\odot < M_b < 10^7 M_\odot$, while for $M_b > 10^7 M_\odot$, we need to reduce the density 100 times for a conservative model compared to Eq. (17). As for the SMBH spin model, the simulations of thin disk accretion find that 70% of SMBHs have extreme initial spin [30]. Thus we assume 70% of SMBHs with initial spin $a = J/GM_b^2 = 0.99$, and we neglect GW signals from other SMBHs with smaller spin. The accretion time is estimated via Salpeter

time [22],

$$t_S = 4.5 \times 10^8 \text{ yr} \frac{\eta}{f_{\text{Edd}}(1-\eta)}. \quad (18)$$

where we take the Eddington ratio $f_{\text{Edd}} = 0.01$ in this work and η is thin-disk radiative efficiency factor [32],

$$\eta = 1 - \sqrt{1 - \frac{2}{3r}}, \quad (19)$$

$$r = 3 + Z_2 - \sqrt{(3 - Z_1)(3 + Z_1 + 2Z_2)}, \quad (20)$$

$$Z_1 = 1 + (1 - a^2)^{1/3}[(1 + a)^{1/3} + (1 - a)^{1/3}], \quad (21)$$

$$Z_2 = \sqrt{3a^2 + Z_1^2}. \quad (22)$$

The SGWB from populated gravitational atom is derived as [31]

$$\Omega_{\text{gwb}}(f) = 0.7 \times \frac{f}{\rho_c} \int dM_b dz \frac{dt}{dz} \frac{d\dot{n}}{dM_b} \frac{dE_s}{df_s}, \quad (23)$$

where f is the frequency of the detector frame, $\rho_c = 3H_0^2/(8\pi G)$ is the critical energy density of the Universe, the Hubble constant $H_0 = 100 h_{100} \text{ km s}^{-1} \text{ Mpc}^{-1}$ with $h_{100} = 0.678$ and dE_s/df_s is the energy spectrum of the radiation in the source frame. We assume $d\dot{n}/(dM_b) = (1/t_0)(dn/dM_b)$ with

$$dt/dz = \frac{1}{H_0(1+z)\sqrt{\Delta(z)}}, \quad (24)$$

where $\Delta(z) = \Omega_M(1+z)^3 + \Omega_\Lambda$, Ω_M is the matter density of the universe and Ω_Λ is the dark energy density.

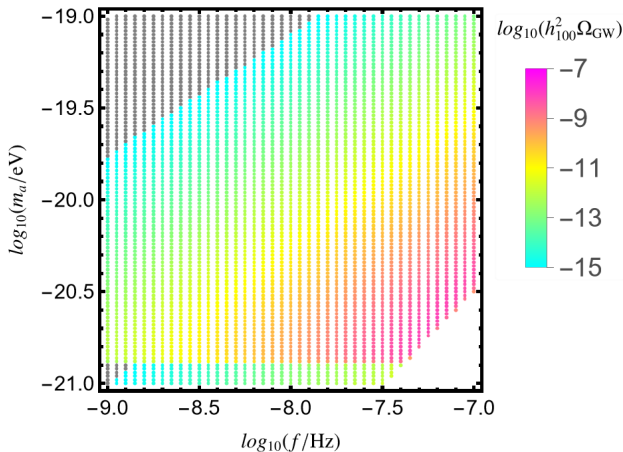


Figure 3. The SGWB energy density from axion transitions between different energy levels with different axion masses and frequencies. The gray region represents the GW strength $h_{100}^2 \Omega_{\text{GW}} < 10^{-15}$ while the blank region depicts no GW signal in the corresponding parameter space.

For discrete frequencies GW spectra, we have

$$\frac{dE_s}{df_s} \approx E_{\text{GW}} \delta(f(1+z) - f_s), \quad (25)$$

where E_{GW} is the radiation energy of the GWs during the signal duration Δt with $\Delta t = \min(\tau_{\text{GW}}, t_0 - t_*, t_S - t_*)$. For the sake of the finite frequency resolution and signal duration of the detector, the Dirac delta function is spread out over a size $\sim \max[1/(\Delta t(1+z)), 1/T_{\text{obs}}]$ [22] where we take $T_{\text{obs}} \approx 15 \text{ yr}$ for PTA. And the radiation energy E_{GW} can be derived from Eq. (16),

$$E_{\text{GW}} = (N_5(t_* + \Delta t) - N_5(t_*)) \Delta \omega. \quad (26)$$

In Fig. 3, we present the predicted GW strength originating from axion transitions between different energy levels in the parameter space of the axion mass and the SGWB frequency. We consider the axion mass range $10^{-21} \sim 10^{-19} \text{ eV}$ and the frequency range $10^{-9} \sim 10^{-7} \text{ Hz}$. For the lighter axion mass region around 10^{-21} eV , since the energy levels we considered in the transition process dominate the GW emission at $1.38 \lesssim \alpha \lesssim 1.85$, only the very large mass BHs could satisfy this requirement. But the superradiant rate is slower for larger BH mass as we can see from Fig. 2, thus these BHs can not produce sufficient axions through the superradiant process to generate observable SGWB strength. For the heavier axion mass region above 10^{-20} eV , the corresponding BHs masses are small. Since the axion occupation number is proportional to the square of the BH mass as Eq. (3), these small mass BHs can not produce enough axions too. Thus the energy-level transitions yield merely feeble GW signals for heavier axion masses.

It is worth noticing that the SGWB from energy-level transition is not monochromatic due to the fact that the astrophysical SMBHs could have a wide mass range. This is very different from the case of the axion annihilation signal where the GW frequency only depends on the axion mass. Moreover, there may exist other transition levels in the axion cloud. Although the corresponding GW strength is small compared to the case considered in this work, they can provide abundant GW signals which may also fit the PTA experiments. And the mass range favored by PTA data is around $10^{-21} \sim 10^{-20} \text{ eV}$ which can be seen from Fig. 3.

To be more clear to see that axion mass range $10^{-21} \sim 10^{-20} \text{ eV}$ is favored by PTA observation, we show the SGWB spectra for different benchmark axion masses in Fig. 4. The curves show that there exists a peak frequency of SGWB and the peak frequency becomes larger when the axion mass increases. The SGWB strength and frequency have a relation $\Omega_{\text{GW}} \propto f^2$ when $f < f_{\text{peak}}$ as shown in Fig. 4. And through the released results of PTA data, we find that the favored axion mass range is approximately around $2 \times 10^{-21} \text{ eV}$, where the red, pink, and violet lines depict the GW spectra for the

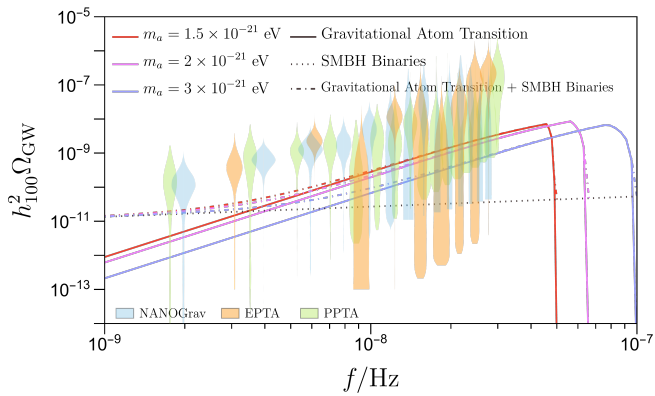


Figure 4. The SGWB spectra from axion transitions between different levels for different axion masses with (dash-dotted lines) and without (solid lines) considering the contributions of SMBH binaries. The red, pink, and violet lines depict the GW spectra for the axion masses of 1.5×10^{-21} eV, 2×10^{-21} eV, and 3×10^{-21} eV, respectively. The black dotted line shows the SGWB spectrum from inspiring SMBH binaries with the prior 2D-Gaussian distribution. The colored violin plots represent the posteriors from the data analyses of different PTA experiments.

axion masses of 1.5×10^{-21} eV, 2×10^{-21} eV, and 3×10^{-21} eV, respectively. The SGWB from axion transitions at low frequency is increased in combination with SMBH binaries. The Bayes factor of the combined SGWB spectra from axion transitions and SMBH binaries for NANOGrav 15-year data is around 1.414 obtained by ENTERPRISE [33] and ENTERPRISE_EXTENSIONS [34] via the wrapper PTArcade [35, 36]. This indicates the axion transitions in combination with SMBH binaries are more favored by NANOGrav 15-year data than SMBH binaries alone. Besides the data released by the NANOGrav, PPTA, and EPTA, the CPTA results also favor the same mass range when considering the SGWB originating from the gravitational atoms. It should be noted that there are other BH mass distribution functions with different power laws and normalization factors that may lead to different results. And for the axion mass around 2×10^{-21} eV favored by PTA experiments concerning the positive power index BH mass distribution model we have used, the SGWB strength is about one-order smaller if we use the negative power index BH mass distribution model. We demonstrate the detailed discussions in the supplemental material.

Conclusion.— We have studied the SGWB from axion transitions between different energy levels composed of the cosmic populated BHs and their surrounding axion clouds formed through the superradiant process. Considering the error bars of the current observation at NANOGrav, EPTA, PPTA, and CPTA data, we found that this type of SGWB can naturally reproduce the observed GW spectra if the axion mass is around

2×10^{-21} eV for the positive power index BH number density distribution function. And for the other representative BH number density distribution function with a negative power index, the axion mass range favored by PTA data is nearly unchanged. The Bayesian analysis shows that the gravitational wave radiated from the transition of the gravitational atom can also explain the GW energy density posterior distributions. The combination of SGWB spectra generated by the gravitational atom transition and the SMBH binaries is more favored for the SGWB from the SMBH binaries.

The only assumption in this work is the existence of ultralight axion particles around 2×10^{-21} eV, which is just the well-motivated fuzzy dark matter. And compared to the well-known interpretations like cosmic string, domain wall, and phase transition, it is less restricted by cosmological constraints and fine-tuning problems since it is formed after the Big Bang nucleosynthesis period. Our work also shows that the PTA experiments can be a novel and realistic approach to probing the superradiance or Penrose process and the isolated black holes. The Hellings-Downs curve is the leading-order term of the overlap reduction function quantifying the correlation between two pulsars. This curve represents the isotropic information, while higher-order terms represent the anisotropic information. The anisotropy analysis at PTA experiments and its deeper implication for the properties of sources are left for our future study [37].

This work was supported by the National Natural Science Foundation of China (NNSFC) under Grant No. 12205387 and Guangdong Major Project of Basic and Applied Basic Research (Grant No. 2019B030302001).

Supplemental Material for “Implication of nano-Hertz stochastic gravitational wave background on ultralight axion particles and fuzzy dark matter”

MASS DISTRIBUTION OF ISOLATED BLACK HOLES

The distribution of isolated black holes (BH) is essential in our calculations. We consider two models of mass distribution as in Refs. [22] and [28],

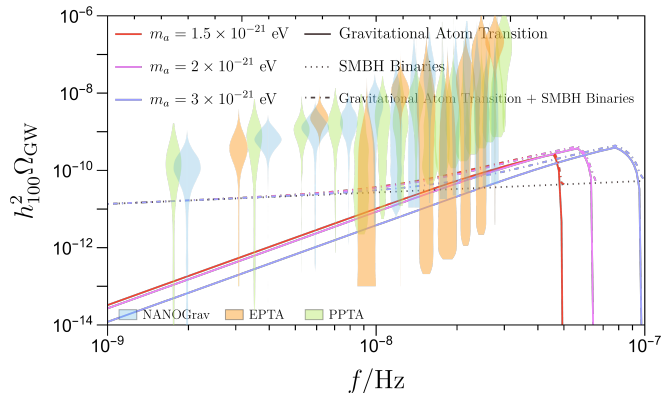


Figure 5. The SGWB spectra from the gravitational atom transition for the PTA favored axion mass range with (dash-dotted lines) and without (solid lines) the super-massive black hole (SMBH) binaries signal. The red, pink, and violet lines depict the GW spectra for the axion masses of 1.5×10^{-21} eV, 2×10^{-21} eV, and 3×10^{-21} eV, respectively. Here we use the negative power index BH mass distribution function, i.e. Eq. (28). The colored violin plots represent the posteriors from the data analyses of different pulsar timing array (PTA) experiments. The black dotted line shows the SGWB spectrum from inspiraling SMBH binaries with the prior 2D-Gaussian distribution.

(1) A positive power index analytic function

$$\frac{dn}{d \log_{10} M_b} = 0.002 \left(\frac{M_b}{3 \times 10^6 M_\odot} \right)^{0.3} \text{Mpc}^{-3}, \quad (27)$$

where M_\odot is solar mass. This formula is used for $10^4 M_\odot < M_b < 10^7 M_\odot$ and $z < 3$, while for $M_b > 10^7 M_\odot$, we need to reduce the distribution 100 times for a conservative model compared to Eq. (27).

(2) A negative power index analytic function

$$\frac{dn}{d \log_{10} M_b} = 0.005 \left(\frac{M_b}{3 \times 10^6 M_\odot} \right)^{-0.3} \text{Mpc}^{-3}, \quad (28)$$

This formula is used for $10^4 M_\odot < M_b < 10^7 M_\odot$ and $z < 3$, while for $M_b > 10^7 M_\odot$, we reduce the distribution 10 times compared to Eq. (28).

We have used the mass function in Eq. (27) to estimate the stochastic gravitational wave background (SGWB) in the main text. And here we give the results of the other

mass function in Eq. (28). The SGWB energy density of different axion masses and frequencies with the negative power index mass distribution function is shown in Fig. 5. The red, pink, and violet lines depict the gravitational wave (GW) spectra for the axion masses of 1.5×10^{-21} eV, 2×10^{-21} eV, and 3×10^{-21} eV, respectively. For the axion mass around 2×10^{-21} eV, the SGWB strength of the negative power index distribution model is nearly one order smaller than the positive index distribution model. We find that the axion mass range favored by PTA data is nearly unchanged for different BH mass distribution models. And the SGWB energy density can be ignored around the typical axion mass range 10^{-22} eV of the fuzzy dark matter for both SMBH distribution models.

* huangfp8@sysu.edu.cn

- [1] R. w. Hellings and G. s. Downs, *Astrophys. J. Lett.* **265**, L39-L42 (1983) doi:10.1086/183954
- [2] G. Agazie *et al.* [NANOGrav], doi:10.3847/2041-8213/acdac6 [arXiv:2306.16213 [astro-ph.HE]].
- [3] J. Antoniadis, P. Arumugam, S. Arumugam, S. Babak, M. Bagchi, A. S. B. Nielsen, C. G. Bassa, A. Bathula, A. Berthereau and M. Bonetti, *et al.* [arXiv:2306.16214 [astro-ph.HE]].
- [4] D. J. Reardon, A. Zic, R. M. Shannon, G. B. Hobbs, M. Bailes, V. Di Marco, A. Kapur, A. F. Rogers, E. Thrane and J. Askew, *et al.* doi:10.3847/2041-8213/acdd02 [arXiv:2306.16215 [astro-ph.HE]].
- [5] H. Xu, S. Chen, Y. Guo, J. Jiang, B. Wang, J. Xu, Z. Xue, R. N. Caballero, J. Yuan and Y. Xu, *et al.* doi:10.1088/1674-4527/acdfa5 [arXiv:2306.16216 [astro-ph.HE]].
- [6] A. Afzal *et al.* [NANOGrav], doi:10.3847/2041-8213/acde91 [arXiv:2306.16219 [astro-ph.HE]].
- [7] J. Antoniadis, P. Arumugam, S. Arumugam, P. Auclair, S. Babak, M. Bagchi, A. S. Bak Nielsen, E. Barausse, C. G. Bassa and A. Bathula, *et al.* [arXiv:2306.16227 [astro-ph.CO]].
- [8] R. D. Peccei and H. R. Quinn, *Phys. Rev. Lett.* **38**, 1440-1443 (1977) doi:10.1103/PhysRevLett.38.1440; S. Weinberg, *Phys. Rev. Lett.* **40**, 223-226 (1978) doi:10.1103/PhysRevLett.40.223; F. Wilczek, *Phys. Rev. Lett.* **40**, 279-282 (1978) doi:10.1103/PhysRevLett.40.279; J. E. Kim, *Phys. Rev. Lett.* **43**, 103 (1979) doi:10.1103/PhysRevLett.43.103; M. A. Shifman, A. I. Vainshtein and V. I. Zakharov, *Nucl. Phys. B* **166**, 493-506 (1980) doi:10.1016/0550-3213(80)90209-6; A. R. Zhitnitsky, *Sov. J. Nucl. Phys.* **31**, 260 (1980); M. Dine, W. Fischler and M. Srednicki, *Phys. Lett. B* **104**, 199-202 (1981) doi:10.1016/0370-2693(81)90590-6; P. Sikivie, *Rev. Mod. Phys.* **93**, no.1, 015004 (2021) doi:10.1103/RevModPhys.93.015004 [arXiv:2003.02206 [hep-ph]].
- [9] P. Svrcek and E. Witten, *JHEP* **06**, 051 (2006)

- doi:10.1088/1126-6708/2006/06/051 [arXiv:hep-th/0605206 [hep-th]].
- [10] J. Preskill, M. B. Wise and F. Wilczek, *Phys. Lett. B* **120**, 127-132 (1983) doi:10.1016/0370-2693(83)90637-8; M. Dine and W. Fischler, *Phys. Lett. B* **120**, 137-141 (1983) doi:10.1016/0370-2693(83)90639-1
- [11] P. Sikivie, *Lect. Notes Phys.* **741**, 19-50 (2008) doi:10.1007/978-3-540-73518-2_2 [arXiv:astro-ph/0610440 [astro-ph]].
- [12] R. Penrose, *Riv. Nuovo Cim.* **1**, 252-276 (1969) doi:10.1023/A:1016578408204
- [13] Zel'Dovich, Ya. B. *Journal of Experimental and Theoretical Physics Letters*, Vol. 14, (1971)
- [14] A. A. Starobinsky, *Sov. Phys. JETP* **37**, no.1, 28-32 (1973)
- [15] S. L. Detweiler, *Phys. Rev. D* **22**, 2323-2326 (1980) doi:10.1103/PhysRevD.22.2323
- [16] R. Brito, V. Cardoso and P. Pani, *Physics*, Lect. Notes Phys. **906**, pp.1-237 (2015) 2020, ISBN 978-3-319-18999-4, 978-3-319-19000-6, 978-3-030-46621-3, 978-3-030-46622-0 doi:10.1007/978-3-319-19000-6 [arXiv:1501.06570 [gr-qc]].
- [17] A. Arvanitaki, M. Baryakhtar and X. Huang, *Phys. Rev. D* **91**, no.8, 084011 (2015) doi:10.1103/PhysRevD.91.084011 [arXiv:1411.2263 [hep-ph]].
- [18] A. Arvanitaki, M. Baryakhtar, S. Dimopoulos, S. Dubovsky and R. Lasenby, *Phys. Rev. D* **95**, no.4, 043001 (2017) doi:10.1103/PhysRevD.95.043001 [arXiv:1604.03958 [hep-ph]].
- [19] M. Baryakhtar, R. Lasenby and M. Teo, *Phys. Rev. D* **96**, no.3, 035019 (2017) doi:10.1103/PhysRevD.96.035019 [arXiv:1704.05081 [hep-ph]].
- [20] P. S. B. Dev, M. Lindner and S. Ohmer, *Phys. Lett. B* **773**, 219-224 (2017) doi:10.1016/j.physletb.2017.08.043 [arXiv:1609.03939 [hep-ph]].
- [21] N. Xie and F. P. Huang, *Sci. China Phys. Mech. Astron.* **67**, no.1, 210411 (2024) doi:10.1007/s11433-023-2172-7 [arXiv:2207.11145 [hep-ph]].
- [22] R. Brito, S. Ghosh, E. Barausse, E. Berti, V. Cardoso, I. Dvorkin, A. Klein and P. Pani, *Phys. Rev. D* **96**, no.6, 064050 (2017) doi:10.1103/PhysRevD.96.064050 [arXiv:1706.06311 [gr-qc]].
- [23] A. Arvanitaki and S. Dubovsky, *Phys. Rev. D* **83**, 044026 (2011) doi:10.1103/PhysRevD.83.044026 [arXiv:1004.3558 [hep-th]].
- [24] R. Brito, V. Cardoso and P. Pani, *Class. Quant. Grav.* **32**, no.13, 134001 (2015) doi:10.1088/0264-9381/32/13/134001 [arXiv:1411.0686 [gr-qc]].
- [25] H. Yoshino and H. Kodama, *PTEP* **2014**, 043E02 (2014) doi:10.1093/ptep/ptu029 [arXiv:1312.2326 [gr-qc]].
- [26] J. Yang and F. P. Huang, *Phys. Rev. D* **108**, no.10, 103002 (2023) doi:10.1103/PhysRevD.108.103002 [arXiv:2306.12375 [hep-ph]].
- [27] S. R. Dolan, *Phys. Rev. D* **76**, 084001 (2007) doi:10.1103/PhysRevD.76.084001 [arXiv:0705.2880 [gr-qc]].
- [28] S. Babak, J. Gair, A. Sesana, E. Barausse, C. F. Sopuerta, C. P. L. Berry, E. Berti, P. Amaro-Seoane, A. Petiteau and A. Klein, *Phys. Rev. D* **95**, no.10, 103012 (2017) doi:10.1103/PhysRevD.95.103012 [arXiv:1703.09722 [gr-qc]].
- [29] J. R. Gair, S. Babak, A. Sesana, P. Amaro-Seoane, E. Barausse, C. P. L. Berry, E. Berti and C. Sopuerta, *J. Phys. Conf. Ser.* **840**, no.1, 012021 (2017) doi:10.1088/1742-6596/840/1/012021 [arXiv:1704.00009 [astro-ph.GA]].
- [30] M. Volonteri, P. Madau, E. Quataert and M. J. Rees, *Astrophys. J.* **620**, 69-77 (2005) doi:10.1086/426858 [arXiv:astro-ph/0410342 [astro-ph]].
- [31] E. S. Phinney, [arXiv:astro-ph/0108028 [astro-ph]].
- [32] Bardeen, J. M., Press, W. H., & Teukolsky, S. A. 1972, *Astrophys. J.*, 178, 347. doi:10.1086/151796
- [33] Ellis, J. A., Vallisneri, M., Taylor, S. R. and Baker, P. T., (2020) Zenodo. doi:10.5281/zenodo.4059815
- [34] Stephen R. Taylor, Paul T. Baker, Jeffrey S. Hazboun, Joseph Simon and Sarah J. Vigeland, (2021) https://github.com/nanograv/enterprise_extensions
- [35] A. Mitridate, (2023) Zenodo. doi:10.5281/zenodo.7876430
- [36] A. Mitridate, D. Wright, R. von Eckardstein, T. Schröder, J. Nay, K. Olum, K. Schmitz and T. Trickle, [arXiv:2306.16377 [hep-ph]].
- [37] Y. Li, F. P. Huang, X. Wang and X. Zhang, *Phys. Rev. D* **105**, 083527 (2022) doi:10.1103/PhysRevD.105.083527 [arXiv:2112.01409 [astro-ph.CO]].